Thin-Film Module Reverse-Bias Breakdown Sites Identified by Thermal Imaging

Preprint

Steve Johnston, Dana Sulas, Harvey Guthrey, Jun Liu, Lorelle Mansfield, Timothy J. Silverman, and Mowafak Al-Jassim
National Renewable Energy Laboratory

Elizabeth Palmiotti and Angus Rockett
Colorado School of Mines

Andreas Gerber
IEK5-Photovoltaics, Forshungzentrum Jülich GmbH

Presented at the 2018 World Conference on Photovoltaic Energy Conversion (WCPEC-7)
Waikoloa, Hawaii
June 10–15, 2018

Suggested Citation
S. Johnston et al., 2018. “Thin-film module reverse-bias breakdown sites identified by thermal mapping: Preprint.” Golden, CO: National Renewable Energy Laboratory. NREL/CP-5K00-70866.

NREL is a national laboratory of the U.S. Department of Energy Office of Energy Efficiency & Renewable Energy
Operated by the Alliance for Sustainable Energy, LLC

This report is available at no cost from the National Renewable Energy Laboratory (NREL) at www.nrel.gov/publications.

Conference Paper
NREL/CP-5K00-70866
June 2018

Contract No. DE-AC36-08GO28308

NOTICE

The submitted manuscript has been offered by an employee of the Alliance for Sustainable Energy, LLC (Alliance), a contractor of the US Government under Contract No. DE-AC36-08GO28308. Accordingly, the US Government and Alliance retain a nonexclusive royalty-free license to publish or reproduce the published form of this contribution, or allow others to do so, for US Government purposes.

This report was prepared as an account of work sponsored by an agency of the United States government. Neither the United States government nor any agency thereof, nor any of their employees, makes any warranty, express or implied, or assumes any legal liability or responsibility for the accuracy, completeness, or usefulness of any information, apparatus, product, or process disclosed, or represents that its use would not infringe privately owned rights. Reference herein to any specific commercial product, process, or service by trade name, trademark, manufacturer, or otherwise does not necessarily constitute or imply its endorsement, recommendation, or favoring by the United States government or any agency thereof. The views and opinions of authors expressed herein do not necessarily state or reflect those of the United States government or any agency thereof.

This report is available at no cost from the National Renewable Energy Laboratory (NREL) at www.nrel.gov/publications.

Available electronically at SciTech Connect http:/www.osti.gov/scitech

Available for a processing fee to U.S. Department of Energy and its contractors, in paper, from:

U.S. Department of Energy
Office of Scientific and Technical Information
P.O. Box 62
Oak Ridge, TN 37831-0062
OSTI http://www.osti.gov
Phone: 865.576.8401
Fax: 865.576.5728
Email: reports@osti.gov

Available for sale to the public, in paper, from:

U.S. Department of Commerce
National Technical Information Service
5301 Shawnee Road
Alexandria, VA 22312
NTIS http://www.ntis.gov
Phone: 800.553.6847 or 703.605.6000
Fax: 703.605.6900
Email: orders@ntis.gov

Cover Photos by Dennis Schroeder: (left to right) NREL 26173, NREL 18302, NREL 19758, NREL 29642, NREL 19795.

NREL prints on paper that contains recycled content.

Thin-Film Module Reverse-Bias Breakdown Sites Identified by Thermal Imaging

Steve Johnston[1], Dana Sulas[1], Elizabeth Palmiotti[2], Andreas Gerber[3], Harvey Guthrey[1], Jun Liu[1], Lorelle Mansfield[1], Timothy J. Silverman[1], Angus Rockett[2], and Mowafak Al-Jassim[1]

[1]National Renewable Energy Laboratory, Golden, CO, 80401, U.S.A.
[2]Colorado School of Mines, Golden, CO, 80401, U.S.A.
[3]IEK5-Photovoltaics, Forschungszentrum Jülich GmbH, Jülich, 52425, Germany

***Abstract* — Thin-film module sections are stressed under reverse bias to simulate partial shading conditions. Such stresses can cause permanent damage in the form of "wormlike" defects due to thermal runaway. When large reverse biases with limited current are applied to the cells, dark lock-in thermography (DLIT) can detect where spatially-localized breakdown initiates before thermal runaway leads to permanent damage. Predicted breakdown defect sites have been identified in both CIGS and CdTe modules using DLIT. These defects include small pinholes, craters, or voids in the absorber layer of the film that lead to built-in areas of weakness where high current densities may cause thermal damage in a partial-shading event.**

***Index Terms* — imaging, photovoltaic cells, photoluminescence, electroluminescence, reliability, accelerated aging, II-VI semiconductor materials, thermal analysis, breakdown voltage.**

I. INTRODUCTION

Partial shading can induce a reverse bias in shaded cells of modules with series-connected cells. When breakdown occurs in localized defects, significant heating due to high current density and power dissipation can permanently damage the device [1]-[2]. The resulting power losses and reduced performance are important long-term degradation concerns for thin-film modules [3]. The electroluminescence (EL) images of Fig. 1 show examples of localized shunts in outdoor-fielded CIGS ($CuIn_xGa_{(1-x)}Se_2$) modules. Dark spots are shunted regions where carriers recombine through non-radiative paths. Brighter regions are typically found adjacent to the dark spots due to higher currents crowding to the shunt locations.

Reverse-bias breakdown in CIGS modules causes damage in the form of "wormlike defects" [4] that appears to initiate at the scribe lines [4]-[5] or within the main fields of the cells [6]. Examples of wormlike defects using photoluminescence (PL) imaging are shown in Fig. 2(a)-(d). Cells that contain defects often have darker PL intensity due to the lower shunt-limited voltage. Thermal imaging using illuminated lock-in thermography (ILIT) is shown in Fig. 2(e)-(f). The wormlike defects are bright and indicate heating as current flows through these shunt defects when voltage is induced by light pulses during the measurement.

We have previously reported a thermal imaging technique that uses limited current during reverse bias to detect the defects that lead to breakdown and permanent damage [7]. Here, we

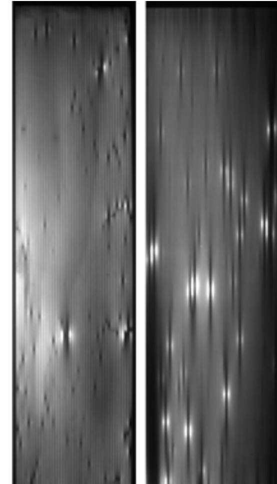

Fig. 1. EL images of modules that have aged and degraded for years in the field. Dark areas show shunt-like defects that result in voltage drops and extension of low EL intensity along the cell near the shunt. Bright areas result from higher current density as carriers crowd toward the shunt defects.

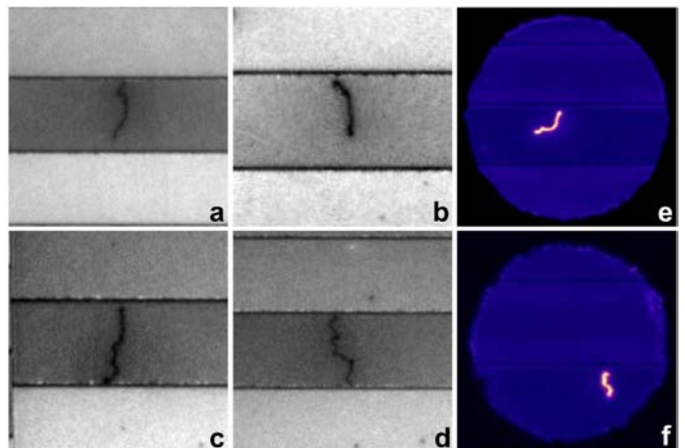

Fig. 2. PL imaging (a)-(d) of shunt defects in the modules from Fig. 1 show long, narrow defect features where material has become damaged and is leading to higher carrier recombination. The decrease in voltage due to the shunts also causes the cell near the defect to emit a lower PL intensity. ILIT imaging (e)-(f) of the defect regions shows that carrier recombination through the shunts results in increased heating.

This report is available at no cost from the National Renewable Energy Laboratory (NREL) at www.nrel.gov/publications.

apply this technique to both CIGS and CdTe to predict early-breakdown defect locations and then track wormlike defect development as current is increased. We show examples of the types of as-grown defects such as voids or pinholes in the absorber layer that instigate early breakdown and wormlike defect formation.

II. Experiment

The mini-modules used in these experiments are either commercial size modules which are cut into smaller sizes or small-scale modules produced with similar processes and architectures of the full-scale module. These samples from various sources have cells that are ~4 to 5 mm wide and ~80 to 100 mm long, and they are characterized by probing across two cells at a time. Dark lock-in thermography (DLIT) images are collected using a Cedip Silver 660M (FLIR SC5600-M) InSb camera with lock-in data acquisition. A Keithley source-meter has been used to apply a large reverse-bias voltage and limit the current. The applied reverse-bias voltage exceeds a sample's breakdown threshold, and the current limit can prevent uncontrolled, thermal runaway damage that leads to wormlike defects or other permanent damage.

III. Results

DLIT imaging shows spatially-resolved heating when currents flow through the device in either forward or reverse bias. An example of uniform current and cell heating of a CIGS sample in forward bias is shown in Fig. 3(a). The current of approximately 15 mA/cm^2 is pulsed at 1 Hz using a square wave. Reverse bias is then applied to this series-connected pair of monolithic CIGS cells within the mini-module. Using a large upper-limit voltage, such as 10 V, with a current-limit of approximately 0.3 mA/cm^2, reverse-bias DLIT indicates heating in localized defects as shown in Fig. 3(b) and 3(c). The zoomed-in view of Fig. 3(c) shows a pre-breakdown defect in the left center of the top cell, another directly below that defect in the middle of the bottom cell, and heating along the scribe lines.

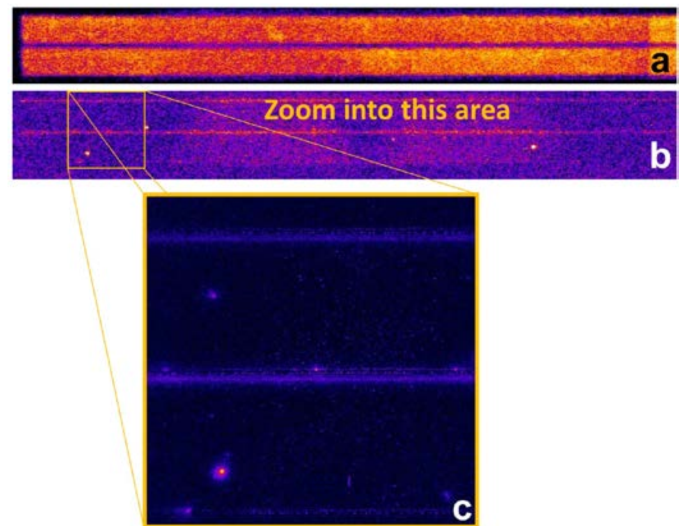

Fig. 3. DLIT imaging shows fairly uniform heating of two series-connected CIGS cells in forward bias (a). With limited current, the reverse-bias DLIT image identifies possible breakdown sites (b). Zooming in for higher spatial resolution shows the location of defects in their pre-breakdown state (c).

Using the zoomed-in field of view of Fig. 3(c), the thermal camera is then set to collect frames for a video, which is not using lock-in thermography. As current is increased in reverse bias, heating in the defects becomes strong enough for the camera to detect it without the need for the averaging and improved signal-to-noise ratio that lock-in acquisition provides. A selection of frames from the reverse-breakdown video are shown in Fig. 4. Frame 1 shows the defects beginning to heat more substantially as the current density is increased to 30 mA/cm^2 when considering the entire cell area. Since current is more concentrated at the defect locations, current density at the defects is significantly larger. Wormlike defects begin to form and propagate in seemingly random directions near the defect origin. After a few seconds, the propagation appears to stop, possibly because the shunted area is now larger and has reduced the current density and heating within the defects. The current limit is increased to roughly 60 mA/cm^2 (full cell area

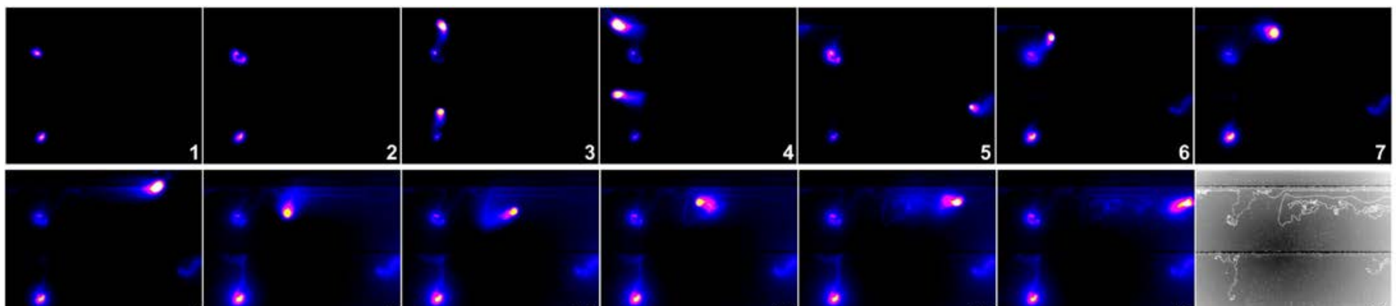

Fig. 4. Selected frames from a thermal camera video show the propagation of wormlike defects during reverse-bias breakdown of the CIGS sample. Frame 1 shows heating at the defects when current density is limited to a low value (30 mA/cm2). Frames 2 and 3 show how the defects begin to propagate when current density is increased to ~60 mA/cm^2. Frames 4 through 13 show how breakdown sustainably travels for roughly a minute within the cells and along scribe lines at a high current density of ~150 mA/cm^2. After stressing, the thermal camera captures the accumulated damage due to breakdown defect propagation as shown in frame 14.

This report is available at no cost from the National Renewable Energy Laboratory (NREL) at www.nrel.gov/publications.

equivalent) and the wormlike defects begin to propagate again, as shown in Fig. 4, frames 2 and 3. At a high current density of ~150 mA/cm^2, breakdown continues to propagate for nearly a minute. As shown in Fig. 4, frames 4 through 13, some trails approach the scribe lines and tend to travel along the scribe lines, suggesting they can sometimes more easily propagate along those features. But, some trails later break away from the scribe lines and either propagate within the field of the cell or once again return toward a scribe line. At this high current density, wormlike defects more sustainably continue to propagate and create damage. A final room temperature thermal image shows the paths of the damage in Fig. 4, frame 14.

The number of wormlike defects and amount of damage have led to some permanent shunting within these cells. A comparison of the before-stress and after-stress current-voltage (I-V) plots are shown in the graph of Fig. 5. After the reverse-bias stress and wormlike defect formation, the I-V curve indicates the cells are significantly shunted.

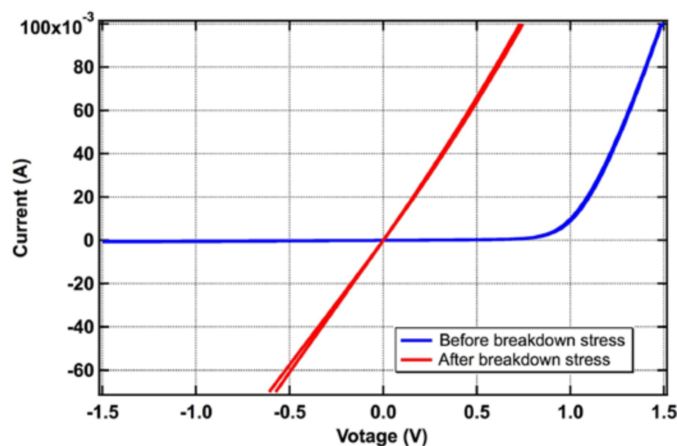

Fig. 5. I-V curves collected before and after reverse-bias stressing are shown for the two series-connected CIGS cells. Reverse-bias breakdown has created permanent shunting within the device.

This breakdown-defect-identification technique is also applied to a CdTe sample. Again, two series-connected cells are imaged using significant reverse bias but with a current limit equivalent to 0.2 mA/cm^2 for the full cell area. A DLIT image is collected as before, and the potential breakdown sites detected using limited current are shown in red color in Fig. 6, frame 1. One defect appears near the center scribe lines on the left half of the image, while a second defect is within the lower cell on the right half of the image. Using this zoomed-in view, the camera is set to collect video and capture the frames with applied reverse bias. With current densities of 20 and 40 mA/cm^2, the defects heat up but do not appear to propagate, as shown in Fig. 6, frame 2. As current is increased to 100 mA/cm^2, the scribe line defect quickly propagates left and right along the scribe line as shown in Fig. 6, frame 3. A third defect appears within the lower cell on the left half of the sample below the scribe line defect. Propagation of these defects does not significantly increase (Fig. 6, frames 4 through 6), as these defects tend to remain rather stationary over time (minutes) with the 100 mA/cm^2 current density limit. A final DLIT image is collected, and the defect heating is shown in red color in Fig. 6, frame 7. The damage done by this reverse-bias stress has led to increased shunting as seen by the before-stress and after-stress I-V curves of Fig. 7.

By limiting current during applied reverse bias, potential early-breakdown sites can be identified before significant heating due to large current densities occurs. This allows for characterization of the types of defects that lead to localized breakdown and wormlike defects. The previous examples have shown that the identified defects became sources and initiation points of thermal damage and wormlike defects when current densities were increased. When only identifying defects with limited current, their structure in their as-grown condition can be preserved and studied to identify the types of defects that exist after cell manufacture.

Cells in both CIGS and CdTe have been stressed only with limited current to identify potential early-breakdown defects. Cross sections of some of these defects have been prepared using a focused ion beam, and the defect area is observed using a scanning electron microscope (SEM). Cross-sectional views

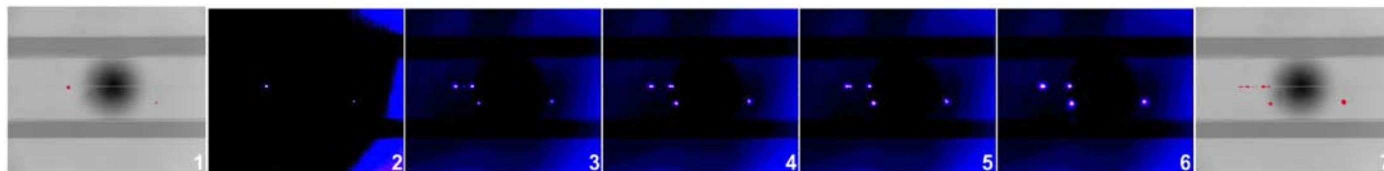

Fig. 6. Selected frames from a thermal camera video show the propagation of defects during reverse-bias breakdown of the CdTe sample. Frame 1 shows the starting current-limited DLIT image in red overlaid on the gray-scale thermal image. The dark spot is due to reflection of the cold camera sensor. Frame 2 shows heating at the defects when current density is limited to a low value (40 mA/cm^2). Frame 3 shows how breakdown travels quickly along the scribe lines, and an additional defect becomes apparent when the current density is increased to ~100 mA/cm^2. Then, frames 4 through 6 show how the defect heating changes rather slowly for roughly a minute. After stressing, the thermal camera captures the accumulated damage due to breakdown defect propagation as shown in frame 7, where the DLIT image in red is overlaid on the gray-scale thermal image.

This report is available at no cost from the National Renewable Energy Laboratory (NREL) at www.nrel.gov/publications.

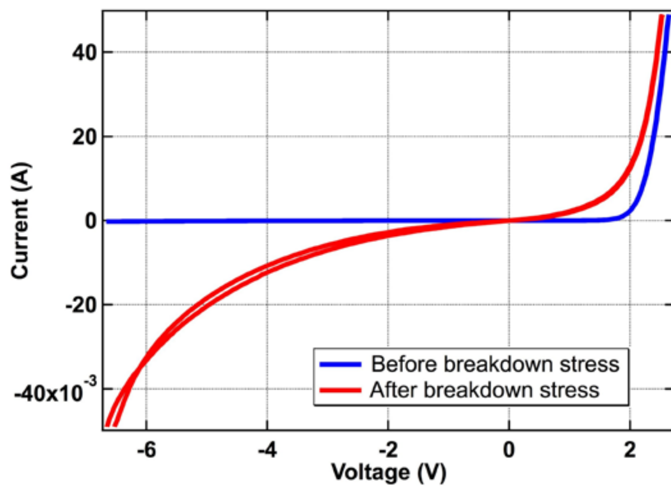

Fig. 7. I-V curves collected before and after reverse-bias stressing are shown for the two series-connected CdTe cells. Reverse-bias breakdown has created permanent shunting within the device.

of potential early-breakdown sites are shown in Fig. 8. The top image, Fig. 8(a), shows the cross-sectional view of a CIGS defect that had appeared as a small pit or pinhole in the surface. This defect is approximately 10 µm in length. The cross section shows a non-uniform absorber layer thickness where there is a void of material and different layers that are likely the top transparent conductive oxide material. This leads to poor device quality in the defect region and likely low device resistance due to the deposition of the top contact material near or on the bottom contact layer. The middle image, Fig. 8 (b), shows a cross-sectional view of an early-breakdown defect in a CdTe sample. This image similarly shows voids and non-uniformities in the absorber layer thickness, and the width of this defect is also roughly 10 µm. Lastly, the bottom image, Fig 8(c), shows a different type of CIGS early-breakdown defect that appears on the surface as a bump or nodule. This defect is about 5 µm in size. The cross-sectional image similarly shows void structures in the absorber film that is common to the other defects.

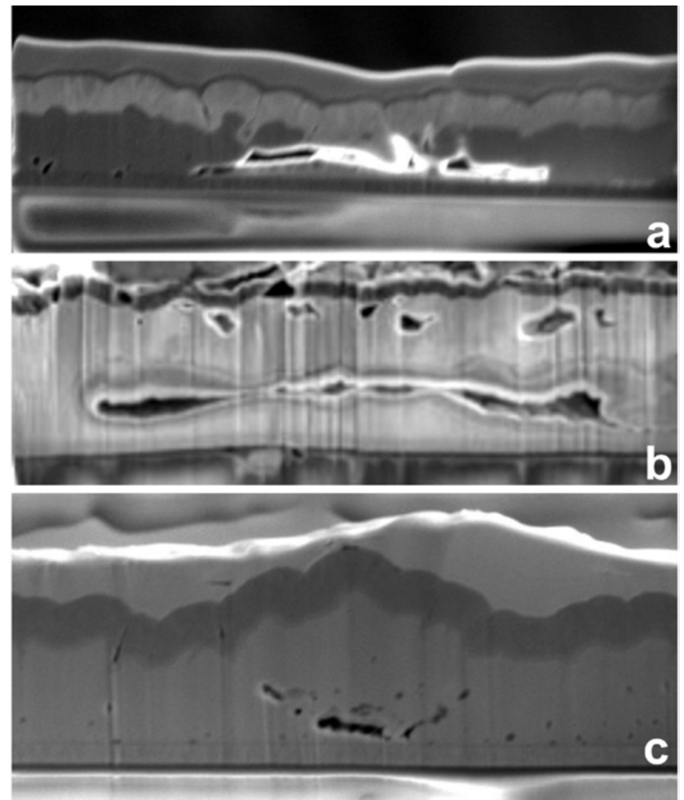

Fig. 8. SEM cross-sectional views show ~10 µm size features associated with the initiation of reverse-bias breakdown. The hole/void type of defects are within the absorber layer of CIGS (a) and CdTe (b). A smaller void-type defect of ~5 µm size shows a curved feature in CIGS (c).

IV. Summary

Partial shading on thin-film modules can lead to degradation when reverse-bias early-breakdown defects cause localized heating and permanent damage. In order to study how these defects are initiated, reverse bias was applied while limiting the current to prevent thermal runaway. DLIT imaging was used to locate sites where heating shows that early breakdown will likely occur. Thermal imaging revealed that the identified defects were the initiating sites for early breakdown, and thermal video recorded the defect propagation. Defects such as film pinholes or voids appear to be weaknesses for reverse bias and may be origins for the formation of wormlike defects under conditions of partial shading.

Acknowledgement

This work was authored in part by Alliance for Sustainable Energy, LLC, the manager and operator of the National Renewable Energy Laboratory for the U.S. Department of Energy (DOE) under Contract No. DE-AC36-08GO28308. Funding provided by U.S. Department of Energy Office of Energy Efficiency and Renewable Energy Solar Energy Technologies Office. The views expressed in the article do not necessarily represent the views of the DOE or the U.S. Government. The U.S. Government retains and the publisher, by accepting the article for publication, acknowledges that the U.S. Government retains a nonexclusive, paid-up, irrevocable, worldwide license to publish or reproduce the published form of this work, or allow others to do so, for U.S. Government purposes. This work was also supported by project DE-EE0007141 of PREDICTS2, and by the German ministry for Economic Affairs and Energy (BMWi) under the contract FK0325724A (OptiCIGS) and by the NREL-Helmholtz "Impuls und Vernetzungsprojekt" HNSEI (SO-075).

This report is available at no cost from the National Renewable Energy Laboratory (NREL) at www.nrel.gov/publications.

REFERENCES

[1] J. W. Bishop, “Microplasma breakdown and hot-spots in silicon solar cells,” *Solar Cell* vol. 26 pp 335-349, 1989.

[2] T. J. Silverman, M. G. Deceglie, X. Sun, R. L. Garris, M. A. Alam, C. Deline, and S. Kurtz, “Thermal and Electrical Effects of Partial Shade in Monolithic Thin-Film Photovoltaic Modules,” *IEEE Journal of Photovoltaics*, vol. 5, no. 6, 2015.

[3] S. Dongaonkar, M. A. Alam, Y. Karthik, S. Mahapatra, D. Wang, and M. Frei, “Identification, Characterization, and Implications of Shadow Degradation in Thin Film Solar Cells,” *IEEE International*, 2011.

[4] E. E. van Dyk, C. Radue, and A. R. Gzasheka, “Characterization of Cu(In,Ga)Se_2 photovoltaics modules,” *Thin Solid Films*, **515**, pp. 6196-6199, 2007.

[5] J. E. Lee, S. Bae, W. Oh, H. Park, S. M. Kim, D. Lee, J. Nam, C. B. Mo, D. Kim, J. Yang, Y. Kang, H. Lee, and D. Kim, "Investigation of damage caused by partial shading of $CuIn_xGa_{(1-x)}Se_2$ photovoltaic modules with bypass diodes," *Prog. Photovolt: Res. Appl.*, 2016.

[6] P. O. Westin, U. Zimmermann, L. Stolt, and M. Edoff, “Reverse bias damage in CIGS module,” *24th European Photovoltaic Solar Energy Conference and Exhibition*, pp. 2967-2970, 2009.

[7] E. Palmiotti, S. Johnston, A. Gerber, H. Guthrey, A. Rockett, L. Mansfield, T. J. Silverman, and M. Al-Jassim, “Identification and analysis of partial shading breakdown sites in $CuIn_xGa_{(1-x)}$ Se_2 modules,” *Solar Energy* **161**, pp. 1-5, 2018.

This report is available at no cost from the National Renewable Energy Laboratory (NREL) at www.nrel.gov/publications.